The role of atmosphere–ocean coupling in the MJO

Steven J. Woolnough

Centre for Global Atmospheric Modelling, Department of Meteorology, University of Reading, Earley Gate, PO Box 243, Reading, RG6 6BB, UK
s.j.woolnough@rdg.ac.uk

ABSTRACT

The observed relationship between convection and sea surface temperature on intraseasonal timescales and the modelled response of an aquaplanet GCM to intraseasonal SST anomalies are discussed with reference to the Madden-Julian Oscillation as a coupled mode of variability. The role of the ocean mixed layer physics and mid-level convection are highlighted as two important processes within the coupled mode which a typically poorly represented in current GCMs.

1 Introduction

The Madden-Julian Oscillation (MJO) is a major source of intraseasonal variability of the tropical circulation and convective precipitation, yet the processes which drive its eastward propagation and determine its period are not well understood. Over the Indian ocean and West Pacific region the phase speed of the MJO is about $5\mathrm{m\,s}^{-}1$, much slower than can be explained by considering the propagation of equatorially trapped Kelvin waves. There have been many attempts to develop a theory of propagation for the MJO centred around the modification of these equatorially trapped Kelvin waves by moist processes, either through the wave-CISK mechanism (e.g. Lau and Peng 1987) or the role of wind-evaporation feedbacks (Emmanuel 1987; Neelin et al. 1987). Both these theories have their weaknesses. The wave-CISK mechanism typically produces disturbances which propagate to quickly and have too small horizontal scales. The evaporation wind feedback mechanisms can produce disturbances which propagate with observed phase speed of the MJO, but still with too small spatial scales. However the major weakness of these evaporation feedback mechanisms is their requirment for basic state surface easterlies in the tropics. In the region where the convective signal of the MJO is large the climatological winds are westerly at the surface.

Observations from the Tropical Ocean Global Atmosphere Coupled Ocean Atmosphere Response Experiment (TOGA-COARE) showed that the sea surface temperature (SST) in the West Pacific was modulated by the passage of the MJO (e.g. Weller and Anderson 1996). Such observations led to speculation that the MJO may be a coupled mode of the atmosphere-ocean system (e.g. Flatau et al. 1997).

For such a coupled mechanism to exist both components of the system must be able to influence each other in a consistent way. The convection associated with the MJO must be able to generate significant SST anomalies and in turn the convection must respond to the presence of the SST anomalies. This paper will demonstrate observational and modelling evidence for both of these links. In section 2 the observed relationship between the convection, SST and surface fluxes will be used to describe the mechanism by which the convection can generate SST anomalies and the important components of the air-sea interaction will be investigated using a 1D mixed layer model. In section 3 the response of the atmosphere to intraseasonal SST anomalies will be investigated using an aquaplanet GCM. In section 4 the prospects for a coupled mode of variability, in light of these relationships will, be discussed.

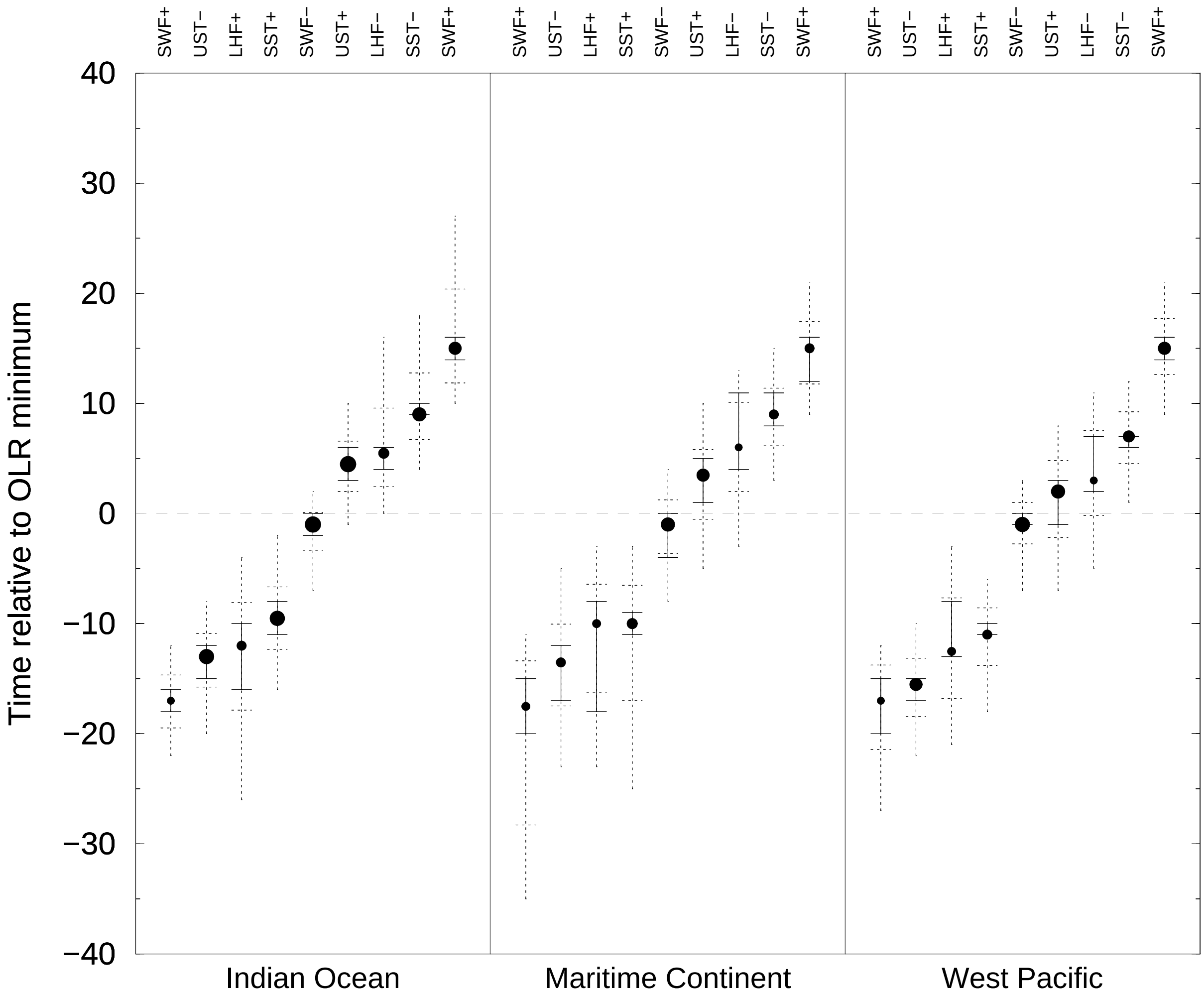

Figure 1: Summary of the temporal relationships between the convection and surface fields (shortwave flux, zonal wind stress, latent heat flux and SST). The dots indicate the lags at which extrema in correlation coefficients occur for 15 years of data. The labels along the top axis indicate the type and sign of the surface anomaly associated with a minimum in OLR (maximum in convection) at the given lag. Taken from Woolnough et al. (2000) (see the article for a full description of the figure)

2 The response of the ocean to the intraseasonal variability in convection

2.1 The large-scale relationship between convection and SST

Figure 1 shows a schematic of the relationship between convection, SST and the surface fluxes taken from Woolnough et al. (2000). It is based on a lag correlation analysis of the 20-100day bandpassed anomalies of Reynolds SST and ECMWF Reanalysis and operational analyses of the surface fluxes and wind stress with the NOAA AVHRR OLR for the period 1982-1997.

Each point on the figure shows the time of significant maximum and minimum lag correlations between each of the surface fields and OLR (as a proxy for deep convection). The dashed error bars give a measure of the both the interannual variability in the relationship between the convection and the surface fields when each MJO season (October-May) is analysed individually and the spatial variability across the regions analysed, the solid error bars indicate the spatial variability across the region when the whole timeseries is analysed at once.

Across the Indian Ocean and the West Pacific out to the date line there is a coherent relationship between the convection and the surface fields on intraseasonal timescales.

About 15-20 days prior to the maximum in convection associated with the active phase of the MJO there are enhanced shortwave fluxes into the surface of the ocean and about 10-15 days before the convection easterly wind stress anomalies. Because of the climatological westerlies in the region these easterly wind stress anomalies lead to a reduction in the evaporation and an additional heat input into the ocean. The combination of the enhanced heat flux into the ocean and the reduced wind stress leads to an increase in the SST with the maximum SST occuring about 10 days prior to the maximum in convection.

Coincident with the maximum in convection there is a reduction in the surface shortwave flux and about 5 days after the convective maximum there are westerly wind stress anomalies and enhanced evaporation. Associated with this reduced heat flux into the ocean the SST cools, with the minimum SST occuring about 10 days after the maximum in convection.

The largest consistent signal of interannual variability in these relationships is associated with ENSO. However, ENSO does not systematically influence the timing of these surface anomalies relative to the convection, but the spatial extent of the region over which this relationship holds. In El Niño years these relationships extend beyond the date line to about 160°W and in La Niña years they do not extend beyond about 160°E consistent with the variations in extent of the westerly winds during El Niño and La Niña.

2.2 The role of the light wind conditions

The light wind conditions which result from the combination of the westerly basic state and the easterly anomalies to the east of (before) the convection play a more important role than simply reducing the evaporation ahead of the convection and thereby producing a positive heat anomaly into the ocean. Figure2 layer shows the SST from two integrations of a 1D mixed layer model incorporating the KPP mixing scheme of Large et al. (1994). The model is forced by surface fluxes and stresses from the IMET buoy at 165°E 1°45'S during the Intensive Observing Period of TOGA-COARE. The control integration shown in the dashed line uses the observed fluxes and wind stresses to force the model. Three periods of intraseasonal warming can be clearly seen (16–24 Nov, 28 Nov–16 Dec, 8–20 Jan), these warming periods coincide with very light wind conditions in the forcing dataset (with the daily mean wind stress $\lesssim 0.02\,\mathrm{N\,m^{-2}}$). The solid line shows the SST from an integration forced by the observed surface fluxes of heat and freshwater, but with the wind stress replaced by the time mean total wind stress for the period ($0.039\,\mathrm{N\,m^{-2}}$). During the light wind phases the SST is significantly underestimated by between 0.5-1°C resulting in intraseasonal SST anomalies of the order of 0.2°C. During these light wind periods the nighttime mixed layer in the control integration is about 10m deep, but in the integration with a fixed wind stress the nighttime mixed layer extends down to about 40m during these periods. The resulting redistribution of the heat gained in the upper few metres during the day to throughout the upper 40m overnight prevents the strong warming of the SST.

As well as reducing the overnight mixing the light wind conditions allow a strong diurnal cycle in SST to develop, the daytime mixed layer is approximately twice as deep in the integration with fixed wind stress compared to the control integration. This reduction in the diurnal cycle accounts for about 0.1°C of the reduction in the intraseasonal warming. The full effect of the diurnal cycle in SST can be seen in figure3. The dotted line shows the SST from the control integration of the 1D model and the dashed line shows the daily mean SST of this integration. The solid line shows the SST from an integration forced by daily mean fluxes. During the light wind periods when the diurnal cycle is large the daily mean SST is approximately 0.3°C higher than in the integration with no diurnal cycle. Because the light wind periods are also the periods in which the intraseasonal SST anomalies are positive this rectification of the diurnal cycle in SST tends to increase the magnitude of the intraseasonal variability in SST. Bernie et al. (2003) found in experiments in a 1D model that to properly capture this diurnal cycle requires an upper layer in the ocean model of the order of 1m thick and a temporal

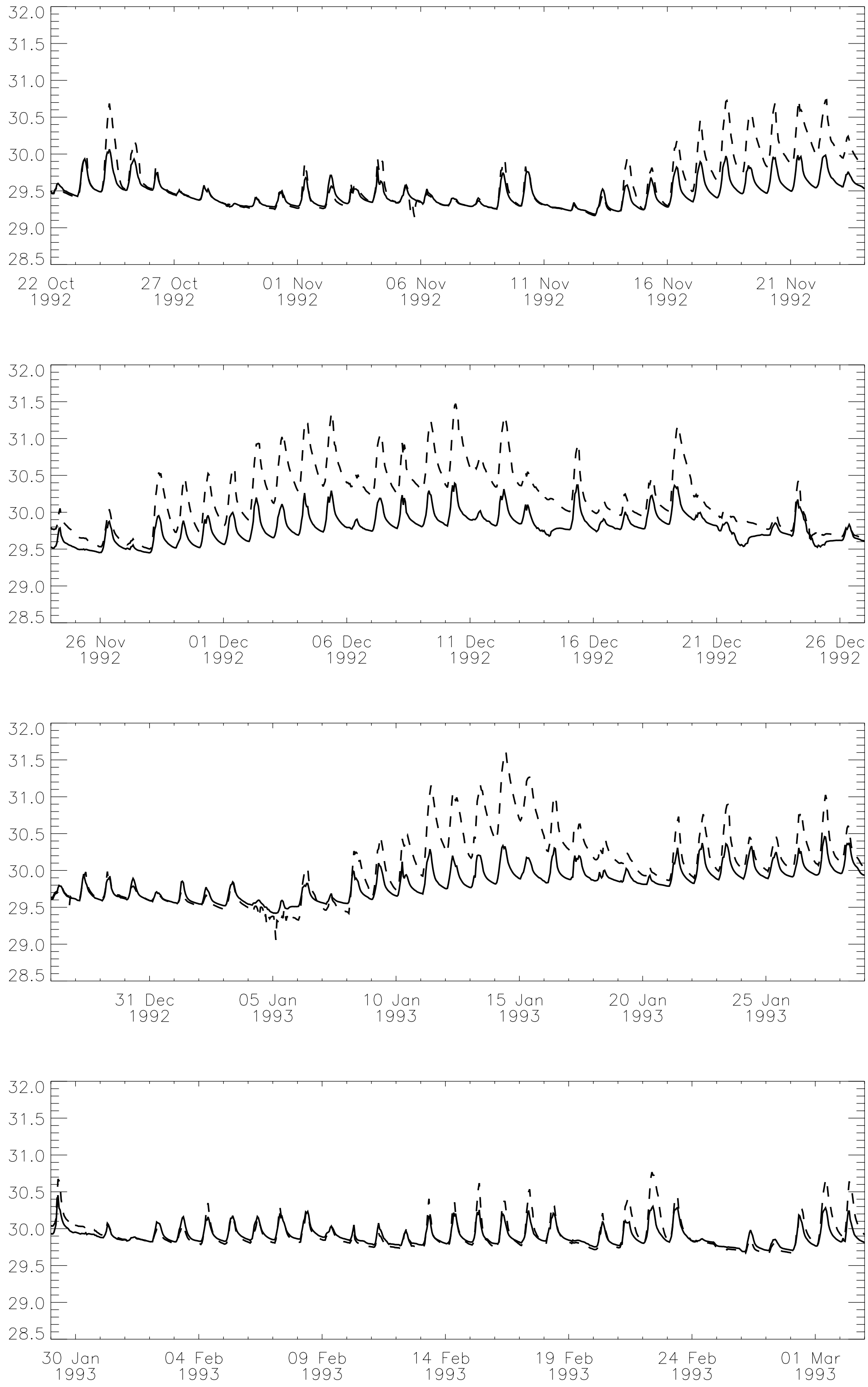

Figure 2: SST from the 1D mixed layer model forced by observed surface fluxes and windstresses from the IMET mooring during the IOP of TOGA-COARE (dashed line) and from an integration with the windstress fixed to the time mean for the period (solid line).

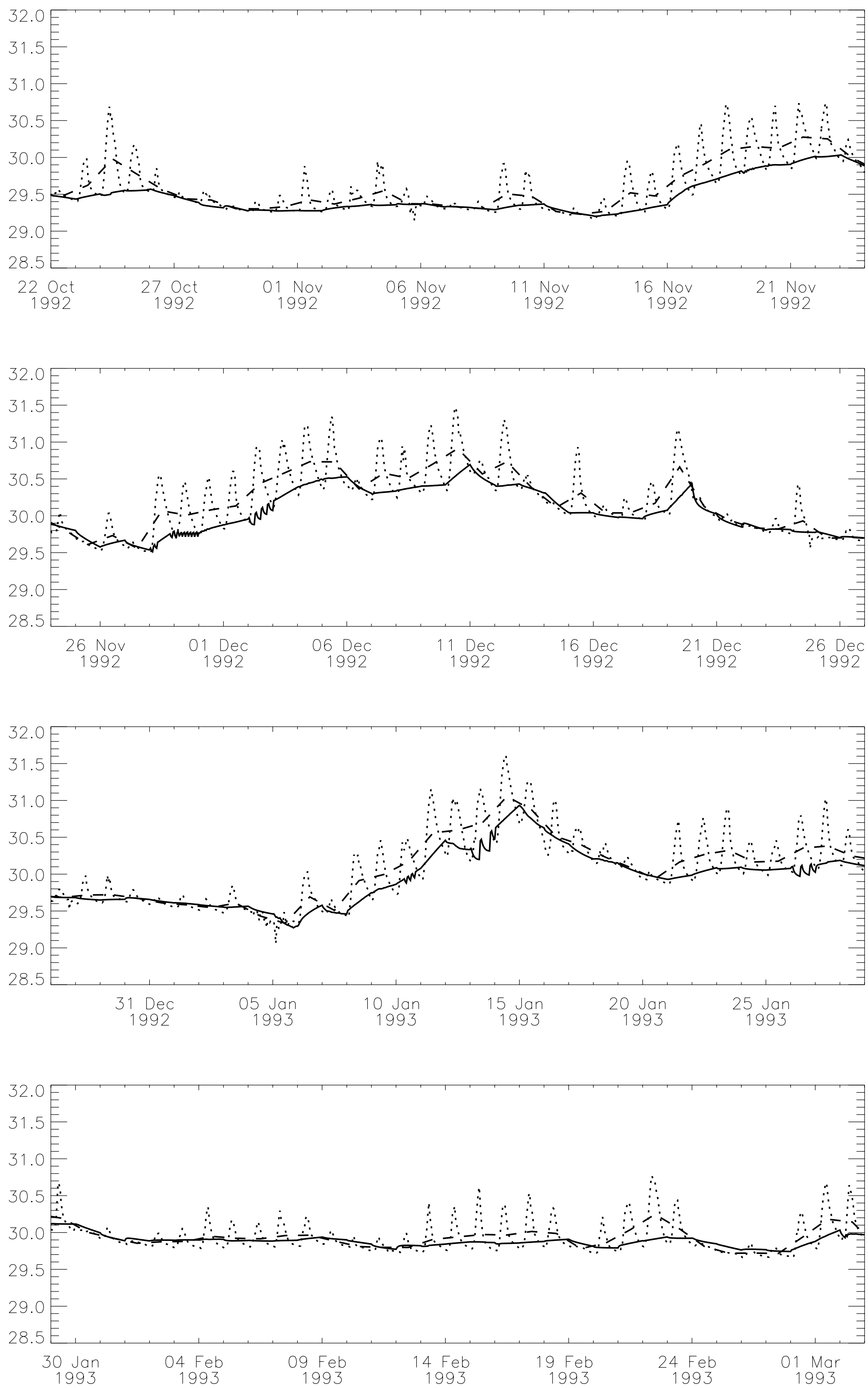

Figure 3: SST from the 1D mixed layer model forced by observed surface fluxes and windstresses from the IMET mooring during the IOP of TOGA-COARE (dotted line), the daily mean SST of this integration (dashed line) and the SST from an integration forced by the daily mean surface fluxes and windstress (solid line).

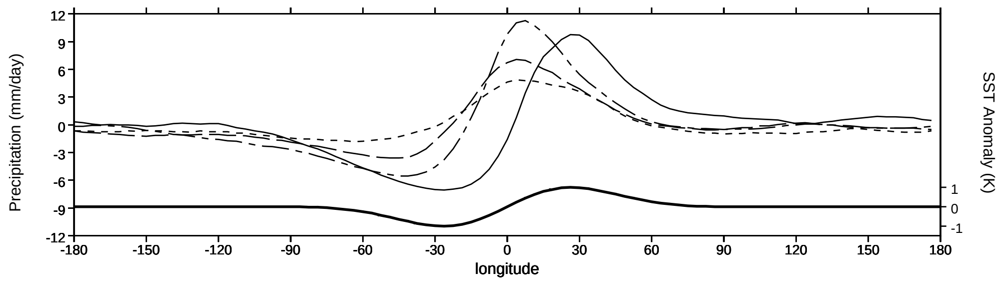

Figure 4: Equatorial precipitation anomaly composited relative to the stationary SST anomaly (solid line) and the SST anomalies moving with speeds equivalent to a period of 90 days (dot-dashed line), 60 days (dashed line) and 30days (dotted line). The thick solid line shows the SST anomaly on the equator. Taken from Woolnough et al. (2001)

flux resolution of about 3 hours. Current coupled GCMs typically have an upper ocean layer of 10m thickness and couple once per day. With such a configuration the intraseasonal variability in the ocean is likely to be underestimated and as such any coupling on intraseasonal timescales will be reduced in these models.

3 The organization of convection by intraseasonal SST anomalies

Figure 4 (from Woolnough et al. 2001) shows the equatorial precipitation anomaly from a series of experiments in an aquaplanet version of the Met Office HadAM3 model forced by a stationary SST anomaly and eastward propagating intraseasonal SST anomalies with speeds of 4,6,12° day^{-1} corresponding to periods of 90,60,30 days respectively. The SST anomalies have a spatial scale and magnitude comparable to the observed SST anomalies associated with the MJO. For the stationary SST anomaly the precipitation maximum is colocated with the SST anomaly, however for the moving SST anomalies the precipitation maximum is shifted westward relative to the SST maximum and lies close to the zero in the centre of the dipole or the maximum in SST gradient. The location of the precipitation anomaly for the moving SST anomalies is consistent with the location of the observed precipitation anomaly associated with the MJO. For the moving SST anomalies the magnitude of the precipitation anomaly is reduced in magnitude as the propagation speed of the SST anomaly is increased.

The location of the precipitation anomalies and analysis of the CAPE and CIN suggests that the precipitation anomalies are not simply a response to the low-level instability generated by the SST anomalies. Figure5 shows longitude-height cross sections of the specific humidity anomaly composited relative to the SST anomalies. In all the integrations the boundary layer humidity anomalies are coincident with the maximum in SST, suggesting that the boundary layer responds quickly to the SST anomaly. However, for the moving SST anomalies, the humidity anomalies in the lower troposphere above the boundary layer are shifted to the west of the SST maximum. Above the freezing level, there is a further westward shift in the maximum humidity anomaly.

Locally, as the SST anomaly increases the boundary layer humidity increases and the low-level instability increases. However, initially the convection generated by this low-level instability passes through relatively dry air in the lower troposphere, and the effect of the entrainment of environmental air is to reduce the buoyancy of the convective parcel and the precipitation efficiency of the convection. The detrainment by the convection and the moistening by the large-scale circulation gradually increases the humidity in the lower troposphere. As this moistening occurs the convection triggered by the low-level instability will encounter an increasingly moist environment, the parcels will dry out less through entrainment and retain their buoyancy excess for longer and generate more precipitation. As the warm SST anomaly moves away the source of low-level instability is removed and the convection and precipitation will begin to decrease. Hence, the location of the precipitation

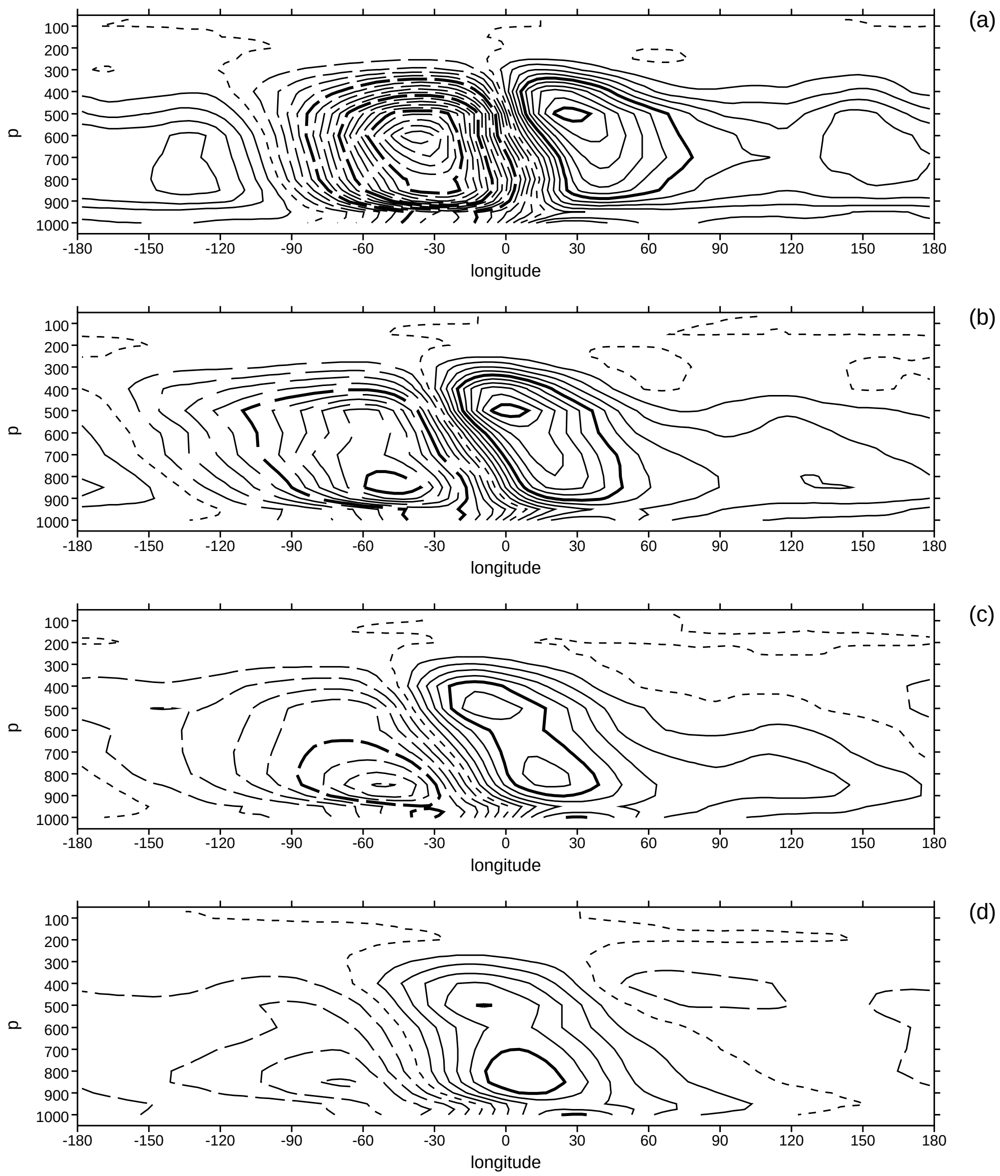

Figure 5: Equatorial cross sections of the specific humidity anomaly from the zonal mean composited relative to the SST anomalies for (a) the stationary experiment and the experiments with moving SST anomalies with speeds equivalent to periods of (b) 90 days, (c) 60days and (d) 30 days. The contour interval is 0.1g kg^{-1}, positive contours are solid, negative contours are dashed and the zero contour is dotted. Heavy contours are multiples of 0.5g kg^{-1}. Taken from Woolnough et al. (2001)

maximum is essentially determined by the spatial structure of the moving SST anomalies and does not vary greatly between each integration. However, the magnitude of the precipitation response depends on the speed of the anomalies since the slower moving SST anomaly can influence the atmosphere for longer, leading to a greater moistening of the free troposphere and larger precipitation anomalies.

The moistening of the free troposphere by the convection clearly plays an important role in determining the response of the convection to the SST. In the real atmosphere the processes which moisten the lower troposphere prior to the onset of the active phase of the MJO are likely to be the shallow and mid-level convection (*cumulus congestus*). Johnson et al. (1999) report a increase of these types of clouds prior to the onset of the active phase of the MJO and an associated deepening of the moist layer in the lower troposphere. Sui et al. (1997) found that these mid-level clouds have a diurnal cycle much more typical of land, with peaks in the late afternoon and early evening, rather than the early morning maximum typical of deep oceanic convection. The strong diurnal cycle in SST during these periods may play an important role in forcing these congestus clouds and hence preconditioning the atmosphere for deep convection.

4 A coupled mode of variability

The results presented in sections 2 and 3 clearly demonstrate that the atmosphere can force the ocean on intraseasonal timescales and that the tropical atmosphere and convection in particular can respond to intraseasonal SST anomalies. Furthermore the phase relationship between the modelled convective response and the SST anomalies is consistent with the observations and the proposed coupled mechanisms.

The sensitivity of the convective response to the period of the SST anomalies will give rise to a preferred timescale for a coupled mode of variability. Slow (fast) moving SST anomalies will generate a large (small) convective response which in turn will have large (small) flux anomalies associated with it. These large (small) flux anomalies are inconsistent with slow (fast) moving SST anomalies.

It is possible to construct a very simple model of the processes involved in this coupled mode of variability to get an estimate of this preferred timescale. Suppose that the SST profile is given by

$$\mathrm{SST} = \Delta T \sin(kx - \omega t), \tag{1}$$

and that the convective response is in quadrature with the SST, proportional to the magnitude of the SST anomaly and inversely proportional to the frequency of the SST anomaly, i.e.

$$\mathrm{PPT} = \alpha \cdot \frac{\Delta T}{\omega} \cos(kx - \omega t). \tag{2}$$

For the purposes of this model we shall assume that the flux variations have the opposite phase to the convection (equivalent to assuming that the shortwave flux anomalies dominate) and proportional to the convective response, i.e.

$$\mathrm{FLUX} = -\beta \cdot \mathrm{PPT}. \tag{3}$$

These equations are linked through an expression for the time variation of the SST,

$$\frac{\partial}{\partial t}\mathrm{SST} = \gamma \cdot \mathrm{FLUX}. \tag{4}$$

Combining equations (1)-(4) gives an expression for the period of oscillation

$$\omega = \sqrt{(\alpha\beta\gamma)} \tag{5}$$

Using estimates of the three constants of proportionality in equations (2)-(4) from observations and modelling studies gives an estimate of the preferred period for the coupled mode. From the aquaplanet results presented in 3 we can estimate $\alpha \sim 0.6\mathrm{mm\,K^{-1}\,day^{-2}}$. Observational studies (e.g. Woolnough et al. 2000; Weller and Anderson 1996) imply $\beta \sim 8\mathrm{W\,m^{-2}/(mm\,day^{-1})}$. Using a mean mixed layer depth of 20m gives $\gamma \sim 1.2 \times 10^{-8}\mathrm{K\,m^2\,J^{-1}}$. Substituting these values into equation (5) gives a preferred period of about 90 days. This period is longer than the observed frequency of the MJO, but reasonable given the relative simplicity of the model.

Modelling a coupled MJO

Some of the important processes in the coupled mode of variability described here are generally not well represented in coupled GCMs.

- The typical vertical resolution in the upper ocean is not sufficient to properly resolve the the diurnal cycle or the shallow mixed layers associated with the break phase of the MJO. Most CGCMs are coupled on a daily basis and as such will have no representation of the diurnal cycle of SST. The absence of this diurnal cycle will not only have a direct impact on the SST variability but may also have implications for the intraseasonal evolution of the mixed layer.
- Mid-level convection is typically not well captured by GCMs which often tend to a bimodal distribution of deep and shallow convection. In part this may be the result of poor vertical resolution (e.g. Inness et al. 2001) but may also arise from weakness in the convective parametrization, e.g. a lack of sensitivity of the convection parametrization to mid-level tropospheric humidity anomalies.

The relatively poor representation of these processes in most coupled GCMs along with errors in the basic state may lead to smaller than expected improvements in the representation of the MJO in coupled GCMs over atmosphere only GCMs.

References

Bernie, D. J., S. J. Woolnough, J. M. Slingo and E. Guilyardi (2003). Modelling diurnal to intraseasonal variability of the ocean mixed layer. *submitted to J. Climate.*

Emmanuel, K. (1987). An Air-Sea Interaction Model of Intraseasonal Oscillations in the Tropics. *J. Atmos. Sci.*, **44**, 2324–2340.

Flatau, M., P. J. Flatau, P. Phoebus, and P. P. Niiler (1997). The feedback between equatorial convection and local radiative and evaporative processes: The implications for intraseasonal oscillations. *J. Atmos. Sci.*, **54**, 2373–2386.

Inness, P. M., J. M. Slingo, S. J. Woolnough, R. B. Neale, and V. D. Pope, 2001: Organisation of tropical convection in a GCM with varying vertical resolution; Implications for the Simulation of the Madden-Julian Oscillation. *Climate Dyn.*,**17**, 777-793.

Large, W. G., J. C. McWilliams, and S. C. Doney (1994). Oceanic vertical mixing: A review and a model with a nonlocal boundary layer parameterization. *Rev. Geophys.*, **32**, 363–403.

Lau, K.-M. and L. Peng (1987). Origin of Low-Frequency (Intraseasonal) Oscillations in the Tropical Atmosphere, Part I: Basic Theory. *J. Atmos. Sci.*, **44**, 950–972

Neelin, J. D. I. M. Held and K. H. Cook (1987). Evaporation-Wind Feedback and Low-Frequency Variability in the Tropical Atmosphere. *J. Atmos. Sci.*, **44**, 2341–2348.

Weller, R. A., and S. P. Anderson (1996). Surface meteorology and air-sea fluxes in the western equatorial Pacific warm pool during the TOGA Coupled-Ocean Atmosphere Response Experiment. *J. Climate*, **9**, 1959–1990.

Woolnough, S. J., J. M. Slingo, and B. J. Hoskins. (2000). The relationship between convection and sea surface temperature on intraseasonal timescales. *J. Climate*, **13**, 2086–2104.

Woolnough, S. J, J. M. Slingo and B. J. Hoskins (2001). The organization of tropical convection by intraseasonal sea surface temperature anomalies. *Quart. J. Roy. Meteor. Soc.*, **127**, 887–908.